Nature Environment and Pollution Technology An International Quarterly Scientific Journal	p-ISSN: 0972-6268 e-ISSN: 2395-3454	Vol. 17	No. 3	pp. 679-690	2018

Original Research Paper | Open Access

Distribution of Soil Water, Salt and Water Drop Penetration Time (WDPT) Under Two-Point-Source Trickle Irrigation with Sewage Water

Yi Li† and Xianze Liu

College of Water Resources and Architecture Engineering, Northwest A&F University, Yangling, Shaanxi, 712100, China

†Corresponding author: Yi Li

Nat. Env. & Poll. Tech.
Website: www.neptjournal.com

Received: 06-10-2017
Accepted: 19-12-2017

Key Words:
Trickle irrigation
Hydrophobicity persistency
Soil water and salt
Wastewater

ABSTRACT

Laboratory two-point-source overlap sewage trickle irrigation experiments were conducted to assess the effects of sewage irrigation rates on soil water repellency, water movement and salt transport. Four flow rates, i.e. 1.08, 2.17, 5.0 and 10.0 mL·min^{-1} were calibrated and applied to three typical soil types. The characteristics, including soil water repellency, wetting patterns and soil salt content distributions were analysed. The results showed that: (1) After short-term (shorter than half a day) sewage irrigation and redistribution, water drop penetration time (WDPT) increased evidently. WDPT increments were the smallest for sand, but the most significant for saline-alkali soil. The larger the flow rates, the longer the WDPTs. (2) The wetting fronts for sand and Lou soils were both smooth, but irregular for saline-alkali soil. Discharge rates of 5 to 10 mL·min^{-1} was suitable irrigation rates for sand and Lou soils. Low application rate (i.e., 1.08 mL·min^{-1} or smaller) was recommended for saline-alkali soil. Power functions were good for quantifying the relationship of horizontal and vertical wetting fronts with respect to time. (3) The distributions of soil salt content and WDPT in horizontal and vertical planes were highly consistent with those of soil water content. Saline-alkali soil with low salt content was found more hydrophobic. In conclusion, short-term sewage trickle irrigation affected distribution of soil water, soil salt and WDPT.

INTRODUCTION

Trickle-irrigation is highly water saving irrigation technique. It is one of the fastest expanding technologies with a great potential for achieving high effectiveness of water-use. It controls greater placement and quantity of water, increases crop yields, and reduces water application as well as fertilizer and cultivation costs. Trickle irrigation has been extensively used in arid lands and desert regions. It performs well for localized salinity management, because soils close to emitters have higher water content and low salt concentration.

Designing trickle irrigation systems involves the selection of a proper combination of trickle discharge rate, spacing between emitters, diameter and length of the lateral system as well as irrigation frequency for any given set of soil, crop and climatic conditions. Soil wetting zones between emitters and the depth-width dimensions of the wetted soil volume were determined and applied in practice. The wetting patterns for different soils at different conditions are complicated such as for deep percolation or under fertigation (Li et al. 2004). The wetted volume formed a 'V'-shaped cross-section in arid soils with surface crust. Soil water content and solute distributions are complicated with the variations of discharge rate. Different models were developed to simulate the soil water dynamics under trickle emitters.

The use of treated wastewater (TWW) in agriculture has been practiced to tackle water crisis. TWW is a valuable source of plant nutrients and organic matter needed for maintaining fertility and productivity levels of the soil (Rusan et al. 2007). The yield was significantly higher with the treated effluent compared with freshwater trickle irrigation. Environmental problems were considered during grey water and sewage water irrigation (Al-Hamaiedeh & Bino 2010). Wastewater disposal practice was environmentally sound compared to its direct disposal to the surface or groundwater bodies. Moreover, clogging of the trickle irrigation system was not a significant problem when TWW was used for irrigation (Al-Nakshabandi et al. 2007).

Water repellent soils are difficult to irrigate and to wet in the range below their critical soil water contents (Dekker & Ritsema 1994; Li & Shang 2016). They are susceptible to preferential flow, which enhances the potential for accelerated leaching to groundwater of hazardous substances. Soil water repellency (SWR) was affected by various complicated factors, including soil moisture variations during wetting and drying process (Doerr & Thomas 2000), soil organic matter (Taumer et al. 2005), temperature (de Jonge et al. 1999), pH (Diehl et al. 2010), etc. In arid zone, water dynamics information in hydrophobic soils is essential for anti-drought of crop. Long-term use with poor-quality

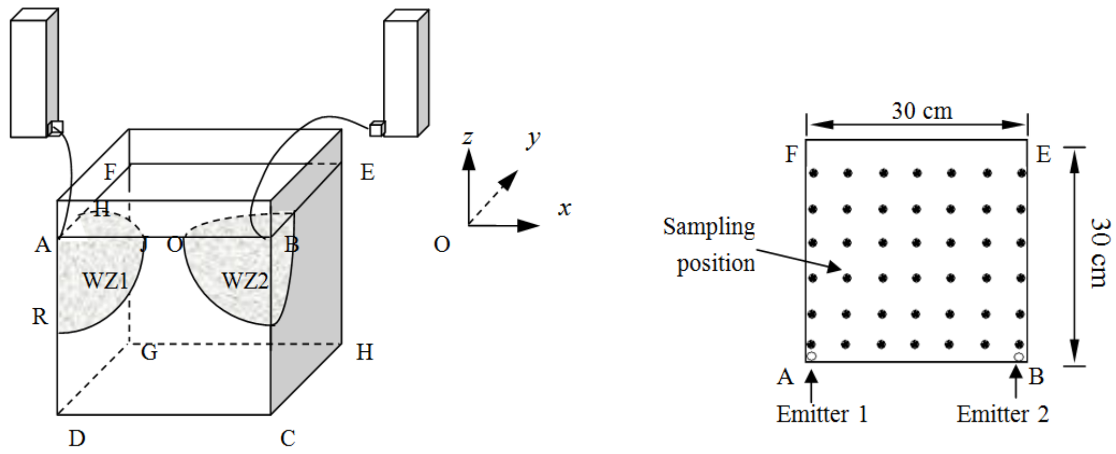

Fig. 1: Experimental system of TTI and sampling scheme. WZ1-wetted zone 1.

wastewater for disposal had led to SWR development (Mataix-Solera et al. 2011). Three-dimensional fingered flow and SWR using a bromide tracer in the field has been studied. Water flow in wettable and water-repellent soils using three different classes of artificial neural networks was conducted. But limited researches were conducted on water, solute and SWR distributions under two-point-source-overlap-TWW-trickle-irrigation (TTI) at present.

As the fast expansion of trickle irrigation in China, the wetting characteristics of soil as well as salt movement and SWR were of much importance because they directly relate to crop yield. This research aims to investigate the effects of various TTI application rates on the distribution of soil water, salt and water drop penetration time (WDPT). This research may reveal phenomena that soil attributes vary related to short term sewage irrigation and propose rational application rates for various soil textures for the field trickle irrigation practice.

MATERIALS AND METHODS

Classification of Hydrophobicity Level

Soil hydrophobicity persistence is tested by the water-drop penetration time (Mataix-Solera et al. 2011). SWR level is classified using WDPT values (Bisdom et al. 1993) (Table 1).

Basic Physico-chemical Characteristics of the Tested Soils

Disturbed sand, Lou soil and saline-alkali soils were collected from top 30 cm depth in Weihe River bank, a crop field in Yangling of Shaanxi province, and a field in Manasi County in Xinjiang, China. The soils were air-dried, ground and sieved by a 2 mm sieve. Initial WDPTs ($WDPT_i$) were measured using a stopwatch by averaging WDPT values of eight water droplets. Soil particle contents were measured with the pipette method. Textures were classified according to the USDA classification system. Soil electrical conductivity (EC) was measured via a DDS-303A conductivity meter. The initial physico-chemical characteristics of the tested soils are listed in Table 2. Saline-alkali soil was considered moderately saline (Luo 1986), while sand and Lou soil were both non-saline soil. Constant-water-head method was used to measure saturated hydraulic conductivity.

Van Genuchten model is used for water retention curves measured by a high-speed centrifuge:

$$\frac{\theta-\theta_r}{\theta_s-\theta_r}=\left(\frac{1}{1+(\alpha h)^n}\right)^m \qquad ...(1)$$

Where, θ, θ_r and θ_s are volumetric, residual and saturated soil water content, $cm^3 \cdot cm^{-3}$; α, n and m are fitted parameters, m=1-1/n. The hydraulic parameters for the tested soils are given in Table 3.

The TWW was collected from Huayu Water Quality Purification Limited Corporation located in the south of Yangling, Shaanxi, China. The initial chemical oxygen demand of the secondary treated TWW was 118.1 $mg \cdot L^{-1}$ (<200 $mg \cdot L^{-1}$ for arid zone), its initial BOD was 71.6 $mg \cdot L^{-1}$ (<100 $mg \cdot L^{-1}$) and initial suspended sediment was 21.1 $mg \cdot L^{-1}$ (<100 $mg \cdot L^{-1}$). Total nitrate was 25.7 $mg \cdot L^{-1}$ and total phosphorus was 3.98 $mg \cdot L^{-1}$, all qualified for farmland irrigation standards in China (GB5084-2005). TWW was filtered to be utilized.

The Laboratory Trickle Irrigation Experiments

TTI experiments were conducted using the equipment systems in Fig. 1. The size of the soil box was 30×30×30 cm^3. There were small 1 mm holes at 3 cm intervals in the box

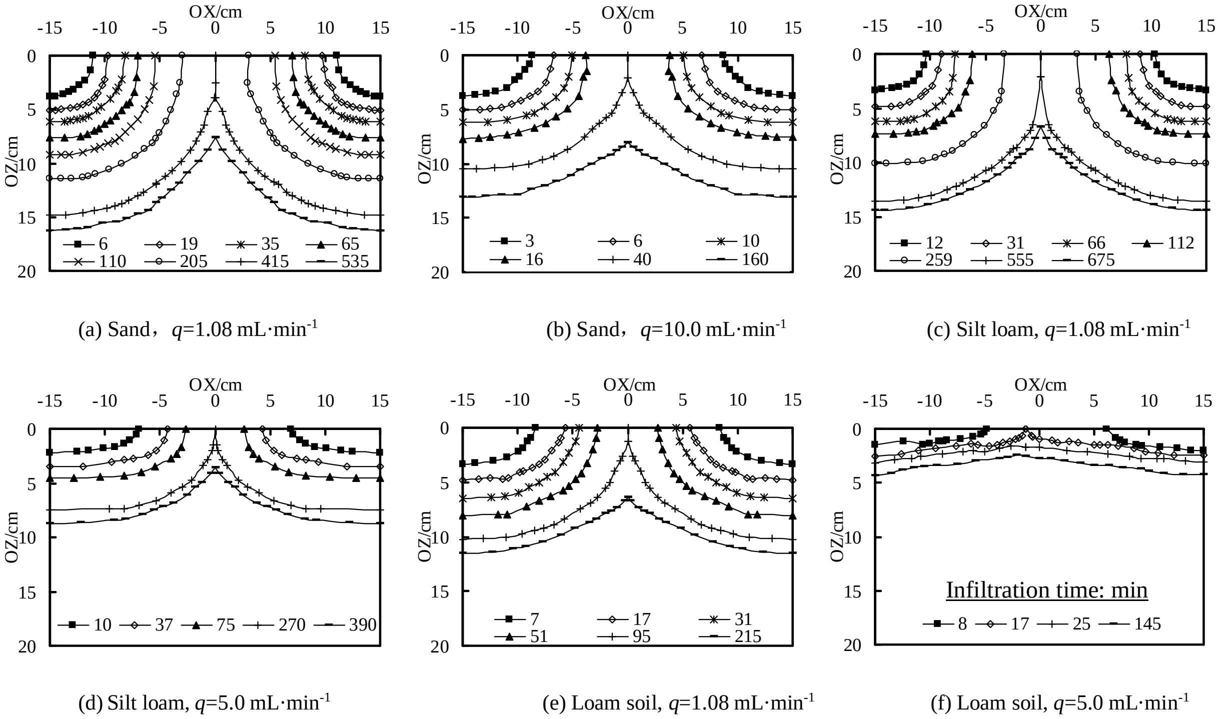

(a) Sand, q=1.08 mL·min^{-1} (b) Sand, q=10.0 mL·min^{-1} (c) Silt loam, q=1.08 mL·min^{-1}

(d) Silt loam, q=5.0 mL·min^{-1} (e) Loam soil, q=1.08 mL·min^{-1} (f) Loam soil, q=5.0 mL·min^{-1}

Fig. 2: Wetting front advances at various application rates q.

bottom wall to ensure no enclosed air in soils. The 5 cm in diameter Marriott bottles filled with TWW were connected with two medical infusion devices to supply water to soils. There was a regulating valve on the infusion device to control the application rates. The needle-heads of the medical infusion device were fixed to the inner corners of the boxes downward rightly 0.5 cm above the soil surface. The spacing between the two emitters was 30 cm. The application rates (q) were pre-calibrated to be 1.08, 2.17, 5.0 and 10.0 mL·min^{-1}, respectively. A q of 10 mL·min^{-1} was not applied to loam soils because of the heavily ponding water and visually irregularity of soil water movement.

The initial soil water content was 0.025, 0.034 and 0.03 cm^3·cm^{-3} for sand, silt loam and loam soil. Soils were packed to the height of 25 cm. A stopwatch was started when the water first dropped to soil surface. Cumulative infiltration was observed from the decreased water level of the Marriott bottle. The wetting front on the XOZ block was visually observed through the box wall.

The experiments were stopped when the wetting fronts overlapped. After two hours of soil water redistribution, soil water moves slower. Soil samples of wetted zone were taken at a 5 cm interval as quickly as possible. Soil water content was measured using oven dry method. Soil samples were grounded and prepared for extract solution using 1:5 ratio of soil to water. Soil saturation extract EC was measured using a DDS-303A type EC meter. EC (µs·cm^{-1}) was correlated to soil salt content (W, g kg^{-1}) measured with the gravimetric method with the relationship W=0.003 EC-1.103 (the coefficient of determination R^2=0.994). WDPT was measured immediately after the soil samples were oven-dried at 75°C, averaged by eight tests. Surfer 8.0 software was applied to draw the contour maps.

Functions for the Wetted Zone

The relationship between wetting fronts and infiltration duration are described with a power function, OX and OZ are correlated to application rate (q, mL·min^{-1}) and t (Li et al. 2004):

$$OX = at^b, OZ = at^b \quad ...(2)$$

$$OX = c(qt)^d, OZ = c(qt)^d \quad ...(3)$$

Where, OX and OZ denote wetting fronts in the horizontal and vertical directions, cm; t represents infiltration time, min; a, b c and d are fitted parameters.

The ratio of horizontal wetting front OX to the vertical wetting front OZ (R_w) indicates the relative infiltration speed in different directions. R_w is described as:

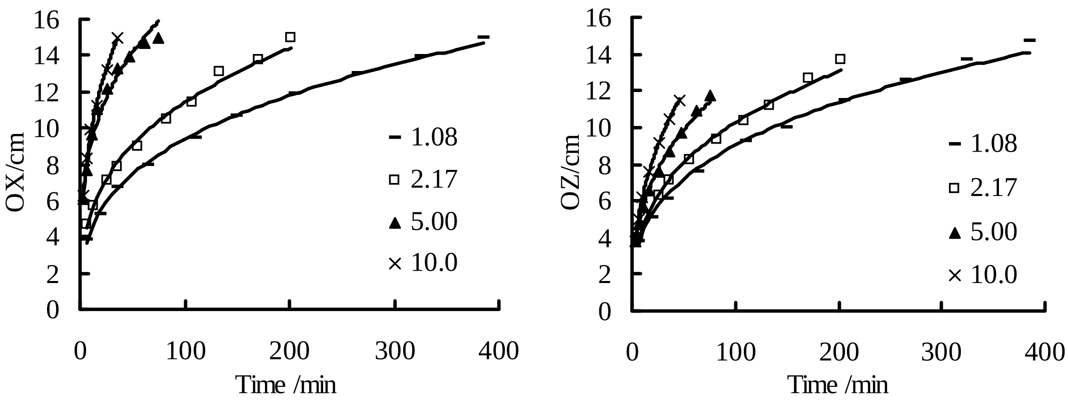

Fig. 3: The advance of wetting front versus application time in horizontal and vertical directions for sand. The legends denote q (mL·min^{-1}).

$$R_w = OX / OZ = et^f \quad ...(4)$$

Where, e and f are fitted parameters. The wetted volume is calculated by using an ellipsoid function:

$$V = V_1 + V_2 = \frac{\pi}{6}(OX_{1,\max} \cdot OY_{1,\max} \cdot OZ_{1,\max} + OX_{2,\max} \cdot OY_{2,\max} \cdot OZ_{2,\max}) \quad ...(5)$$

Where, V is the volume of the whole wetted zone; OX_{max}, OY_{max} and OZ_{max} are the maximal wetting lengths from the origin (point O in Fig. 1a) in the x, y and z directions.

RESULTS

Wetting Front Advances During TTI

The wetting fronts on the YOZ plane were read through the soil box wall during TTI. Wetting fronts on the XOZ quadrant were similar with those on the YOZ plane because the soils were homogeneous and the anisotropy was neglected. Fig. 2 demonstrates the advances of wetting front versus time for the tested soils at various application rates (q).

In Figs. 2a and 2b for sand, the wetting area was almost in a 1/4 circle shape with almost equal infiltration lengths at both horizontal and vertical directions, especially at q of 1.08 mL·min^{-1}. According to observation data of all four application rates, the overlap time for the wetting area was 408, 314, 71 and 36.5 min corresponding to q of 1.08, 2.71, 5.0 and 10.0 mL·min^{-1}. As q increased, the overlap time decreased, but soil water movement in the horizontal direction was a little bit faster than that in the vertical direction. For silt loam (Figs. 2c and 2d), the wetting area presented an ellipse shape. At larger q, when water gradually ponded on soil surface, the horizontal wetting front advanced faster than the vertical one and the wetting area seemed like half an oval. For loam soil (Figs. 2e and 2f), even at q of 1.08 mL·min^{-1} there was ponding water on soil surface. At a larger q of 5.0 mL·min^{-1}, water ponding was observed at soil surface. The wetting front turned to be more irregular, and there was more water flow horizontally, but less water infiltrated downward. The wetting area in XOZ block was more like a rectangle as the two wetted zones overlapped. Under the same q, the wetted zone for loam soil were obviously different with the other two. Large q of 5.0 and 10.0 mL·min^{-1} during TTI was recommended for sand and silt loam, but small q of 1.08 mL·min^{-1} was recommended for loam soil in order to prevent heavy water ponding on soil surface.

The advance of wetting fronts versus time for sand at various q are demonstrated in Fig. 3. Curves for silt loam and loam soil were not shown. When t was fixed, the wetting front curves were elevated as q increased, either in horizontal or vertical directions.

The relation between wetting radius (both horizontal and vertical) and infiltration time t was fitted using Eq. (2). The parameters a and b for various soils at different q are presented in Table 4.

In Table 4, parameter a varied according to the soils, the directions, and the application rates. The coefficients of determination (R^2) were all greater than 0.97, indicating the good correlations of wetting fronts versus time using power functions. When compared in horizontal and vertical directions, the parameters a and b differed small for sand, large for silt loam, and a lot for loam at different q. Li et al. (2004) showed an increasing a at a larger q, but with an almost constant b, both for horizontal and vertical directions for a sandy soil. But b of this research varied with various q.

Table 1: Classification of water repellency according to *WDPT* values.

Level	0	1	2	3	4	5	6	7	8	9
WDPT(s)	<5	6-10	11-30	31-60	61-180	181-300	301-600	601-900	901-3600	>3600

Table 2: The initial soil physico-chemical characteristics. The particle size of clay, silt and sand ranges from < 0.001 mm, 0.001~0.05 mm and 0.05~0.2 mm, respectively. BD-bulk density.

Soil	Clay (%)	Silt (%)	Sand (%)	Soil texture	$WDPT_i$ (s)	EC ($\mu s \cdot cm^{-1}$)	OMC ($g \cdot kg^{-1}$)	BD ($g \cdot cm^{-3}$)
Sand	0.1	6.2	93.7	Sand	1.2	38.7	5.69	1.60
Lou soil	14.8	78.7	6.5	Silt loam	1.6	19.2	7.59	1.35
Saline-alkali	22.8	31.9	45.3	Loam	3.5	623.7	7.38	1.45

Table 3: Parameters of van Genuchten model and hydraulic conductivities for the tested soils. K_s - saturated hydraulic conductivity. *RMSE* - the root mean square error of the fitting.

Soil	θ_r	θ_s	α (cm^{-1})	n	m	R^2	*RMSE*	$K_s \times 10^{-4}$ (cm min^{-1})
Sand	0.02	0.386	0.0509	1.3487	0.2585	0.996	0.0836	206.0
Lou soil	0.08	0.500	0.0144	1.2680	0.2114	0.998	0.0896	43.1
Loam	0.06	0.41	0.0053	1.2658	0.2100	0.995	0.0989	1.96

Table 4: The fitted parameters of the relationship between wetting fronts and infiltration time using Eq. 1 at different application rates (q) and directions for the tested soils.

Soil	Dependent variable	q ($mL \cdot min^{-1}$)	a	b	R^2
Sand	OX	1.08	2.040	0.331	0.998
		2.17	2.456	0.334	0.992
		5.0	4.662	0.284	0.985
		10.0	4.428	0.339	0.997
Silt loam	OX	1.08	2.009	0.317	0.996
		2.17	3.727	0.258	0.989
		5.0	3.761	0.302	0.993
		10.0	6.052	0.268	0.999
Loam	OX	1.08	5.155	0.197	0.996
		2.17	7.663	0.134	0.998
		5.0	5.317	0.367	0.998
Sand	OZ	1.08	1.972	0.330	0.994
		2.17	2.055	0.349	0.997
		5.0	2.463	0.354	0.993
		10.0	2.401	0.410	0.999
Silt loam	OZ	1.08	1.363	0.364	0.999
		2.17	1.293	0.405	0.998
		5.0	1.397	0.442	0.999
		10.0	1.279	0.537	0.996
Loam	OZ	1.08	0.917	0.374	0.994
		2.17	0.769	0.409	0.993
		5.0	0.920	0.366	0.979

The product of application rate and time (qt) represent the volume applied. The fitted parameters for Eq. (3) are presented in Table 5 for the three tested soils. OX and OZ were both proportional to qt with power values d ranging from 0.17 to 0.39. Bar-Yosef & Sheikholslami (1976) reported d of 0.33 for clay and Li et al. (2004) gave d values around 0.33 of OX and 0.45 of OZ for sand and loam. Different soils with different physical properties had various c and d values.

For further comparisons of wetting pattern for the wetted zones, wetting ratio R_w in Eq. (4) was calculated for various q at two directions of the tested soils. Eq. (4) fitted

Table 5: The fitted parameters for relationship between wetting fronts and (qt) using Eq. 2.

Soil type	Dependent variable	c	d	R^2
Sand	OX	2.18	0.322	0.939
Silt loam	OX	2.48	0.290	0.908
Loam	OX	5.76	0.172	0.957
Sand	OZ	1.59	0.340	0.903
Silt loam	OZ	1.00	0.387	0.880
Loam	OZ	0.66	0.389	0.706

well for silt loam and loam, but bad for sand. The shapes of the vertical wetting plane were close to circles for sand. The average R_w ($R_{w,ave}$) and the fitted e and f are given in Table 6. The average R_w increased as application rate increased for both silt loam and loam soil. Large $R_{w, ave}$ existed for loam soil even at small q of 1.08 mL·min^{-1} compared with silt loam and sand, indicating large differences between horizontal and vertical wetting fronts. Parameter e was relatively small for silt loam, but large for loam soil, also indicating the magnitude of differences between the horizontal and the vertical wetting fronts for the different soils. Parameter f ranged between -0.051 and -0.278 with R^2 > 0.87.

The Spatial Distributions of Soil Water Content

The contour maps of soil water content (θ) at various q in the horizontal plane (XOY) and the vertical block (XOZ) for different soils are illustrated in Figs. 4 and 5.

For sand, at the locations below the two emitters, there were maximal θ values. θ decreased along the radial distance from the emitters and reached its minimum at the wetting front. For silt loam, the spatial distributions of θ were almost similar to those of sand at different q, but θ at the locations below the two emitters were larger than those of sand. The contour lines for silt loam were not as smooth and regular as sand. For loam soil, θ also decreased along radial distance from the emitters. However, the wetting zone generally took non-circular shapes. Especially at a large q, the contour map was much irregular, ponding water was observed soon after irrigation started. The overlapped lengths in the middle of the two wetting body were smaller compared to those of sand and silt loam at a given q. Water in loam soils was difficult to infiltrate and ponded at the soil surface easily, resulted in the non-uniformity of θ distribution.

Spatial distributions of θ in XOZ block were different from those in XOY plane (Fig. 5). The contour maps of θ for sand were more regular and shaped like 1/4 ellipse at all q. Similar features were found for silt loam at q of 1.08 mL·min^{-1}. The contour maps of θ for silt loam at a large q and for loam soil at a small q were shaped like flat ellipse with obviously different OX and OZ. The contour maps of θ for loam soil at a large q were shaped like rectangles, the contour lines were horizontally arrayed under these circumstances.

The wetted volume V was calculated using Eq. (5) (Table 7), despite wetted zone for loam soils did not looked ellipse. V increased with q, t and the product of q and t. V was correlated as a power function of (qt):

$$V = 4.736\,(qt)^{1.081},\ R^2 = 0.9125,\ n=11$$

The index 1.081 was close to 1, which means V was almost proportional to the qt.

The average soil water content, θ_{ave}, was calculated using the total infiltration divided by the total volume for each soil. θ_{ave} varied from 0.21 to 0.24 cm^3·cm^{-3} at different q for sand, from 0.283 to 0.299 for silt loam, and was about 0.29 for saline alkali soils.

Effects of TTI on the Distributions of Soil Salt Content

The contour maps of W after TTI at various q values in XOY and XOZ blocks are shown for the tested soils (Fig. 6).

Generally, the distributions of soil salt followed the distributions of soil water. There was the lowest W of soils below the two emitters; slightly larger W was around them. The largest W was distributed at the edges of wetting front. At the locations with high θ, there was low W, showing the leaching salt effects by TWW trickle irrigation. The low initial W for sand and silt loam resulted in responding low W distributions both in XOY and XOZ blocks after TTI, with the highest W being smaller than 0.5 g·kg^{-1} of the wetted zone. But there was large W for loam soil, both in XOY and XOZ blocks at various q values. The largest W for loam decreased from 12.6 to 12.4 and to 7.35 g·kg^{-1} as q increased from 1.08 to 2.17 and to 5.0 mL·min^{-1}.

The Effects of TTI on Potential Soil Water Repellency

The distributions of WDPT on the horizontal plane of XOY: Potential water repellency for measurement was termed on dried soil samples (Dekker & Ritsema 1994). In order to compare the influence of q differences on potential water repellency, contour maps of WDPTs in the XOY plane are shown for the tested soils (Fig. 7).

TWW irrigation had appreciable effects over the water repellency of loam and silt loam soil. For sand, after TTI and short-time redistribution, WDPTs of the wetted zone increased apparently for different q compared to the initial conditions, but none exceeded 5s, indicating the hydrophobicity level of sand did not change, maintaining in level 0 and being hydrophilic. For silt loam, WDPTs of the wetted zone also increased after TTI and short-time redistribution.

Table 6: The fitted parameters of relationship between R_w and t using equation 4 for two soils.

Soil	q (mL·min^{-1})	$R_{w,ave}$	e	f	R^2
Silt loam	1.08	1.18	1.49	-0.051	0.878
	2.17	1.61	2.88	-0.147	0.928
	5.0	1.66	2.69	-0.140	0.936
	10.0	2.32	4.73	-0.269	0.980
Loam	1.08	3.30	7.56	-0.198	0.953
	2.17	4.79	13.0	-0.278	0.986
	5.0	7.07	9.75	-0.133	0.996

Table 7: The calculated total wetted volume, V. $OX_{i,max}$- maximal wetting length in direction x for the ith wetted zone, i=1 and 2, $OX_{1,max}$= $OX_{2,max}$= 15 cm. $OY_{1,max}$- maximal wetting length in direction y for the ith wetted zone. θ_{ave}- average soil water content for the wetted volume.

Soil	q(mL·min^{-1})	t(min)	$OY_{1,max}$(cm)	$OZ_{1,max}$(cm)	$OY_{2,max}$(cm)	$OZ_{2,max}$(cm)	V(cm^3)	θ_{ave}(cm^3· cm^{-3})
Sand	1.08	415	16.8	16.4	16.6	16.2	4276.0	0.210
	2.17	220	17.3	15.4	17.1	15.6	4187.6	0.228
	5	75	15.6	13.5	17.2	13.7	3504.8	0.214
	10	40	17.6	13.1	17.3	13.2	3604.3	0.236
Silt loam	1.08	555	17.5	14.3	17.3	14.6	4202.2	0.285
	2.17	240	17.4	13.5	17.2	13.5	3668.6	0.284
	5	98	17.1	12.2	17.1	12.2	3277.0	0.299
	10	34	14.8	9.8	16.6	9.7	2403.8	0.283
Loam	1.08	280	15.8	8.3	16.1	8.2	2066.9	0.292
	2.17	150	19.2	7.2	19.7	7.3	2215.2	0.294
	5	25	16.9	3.3	16.8	3.2	860.2	0.291

Table 8: The increment of WDPTs after treated TWW trickle irrigation. ΔWDPT, $WDPT_a$ and $WDPT_{max}$- increased, average and maximal WDPTs of the wetted zone, T_O-time when two wetted zone overlapped, T_T-total irrigation time, Q_Z- irrigation quota for single wetted zone.

Soil	q(mL·min^{-1})	T_O(min)	T_T(min)	Q_Z(mL)	$WDPT_i$(s)	$WDPT_a$(s)	$WDPT_{max}$(s)	ΔWDPT(s)
Sand	1.08	408	415	448	1.2	2.1	2.6	0.9
	2.17	214	220	477	1.2	2.7	3.3	1.5
	5.0	71	75	375	1.2	2.3	2.9	1.1
	10.0	36.5	40	400	1.2	2.0	2.5	0.8
Silt loam	1.08	555	555	599	1.6	4.7	6.7	3.1
	2.17	233	235	510	1.6	4.0	6.8	2.4
	5.0	95	95	475	1.6	3.4	6.1	1.8
	10.0	30	30	300	1.6	3.3	5.9	1.6
Loam	1.08	270	270	292	3.5	6.1	11.3	2.6
	2.17	140	140	304	3.5	10.1	23.8	6.6
	5.0	23	25	125	3.5	7.6	10.1	4.2

Especially, WDPTs for the positions below the two emitters increased obviously and were larger than 5s. The hydrophobicity level of partial wetted zone changed from level 0 to level 1, becoming hydrophobic. The increase in WDPT at the locations below emitters suggested that longer TWW irrigation time and larger TWW irrigation quota may cause higher WDPTs. There were obvious low WDPT at the overlapped zone under both q. The contour maps of WDPT were circularly focused around the soils rightly below two emitters. As the distance from the emitters increased, WDPTs decreased gradually. WDPTs of the wetted zones generally showed increased SWR compared to the non-wetted zones. For loam soil, WDPTs of the wetted zone increased significantly. At most wetted locations the WDPTs were above 5 s. At several positions directly below the emitters, WDPTs were beyond 10 s. The maximal WDPT was located near the emitters. The hydrophobicity level of most wetted zone changed from level 0 to levels 1 and 2, becoming hydrophobic.

The distributions of WDPT on the horizontal plane of XOZ: Contour maps of WDPTs at various q in XOZ block are shown in Fig. 8.

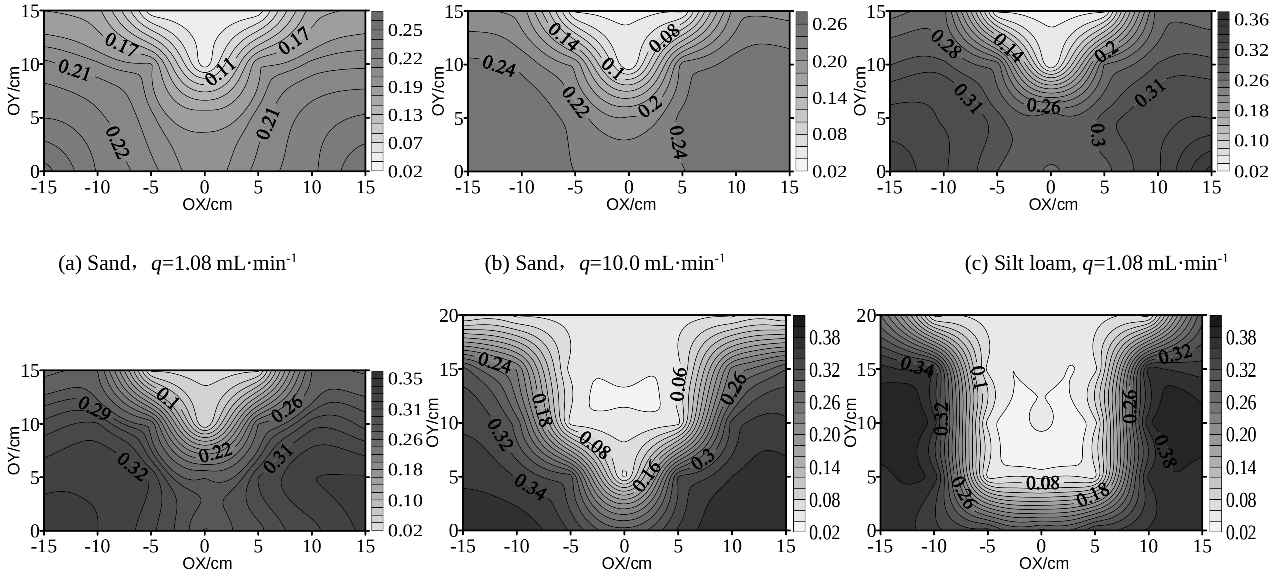

(a) Sand, q=1.08 mL·min[-1] (b) Sand, q=10.0 mL·min[-1] (c) Silt loam, q=1.08 mL·min[-1]

(d) Silt loam, q=5.0 mL·min[-1] (e) Loam soil, q=1.08 mL·min[-1] (f) Loam soil, q=5.0 mL·min[-1]

Fig. 4: Contour maps of θ ($cm^3\ cm^{-3}$) on the XOY plane after TTI.

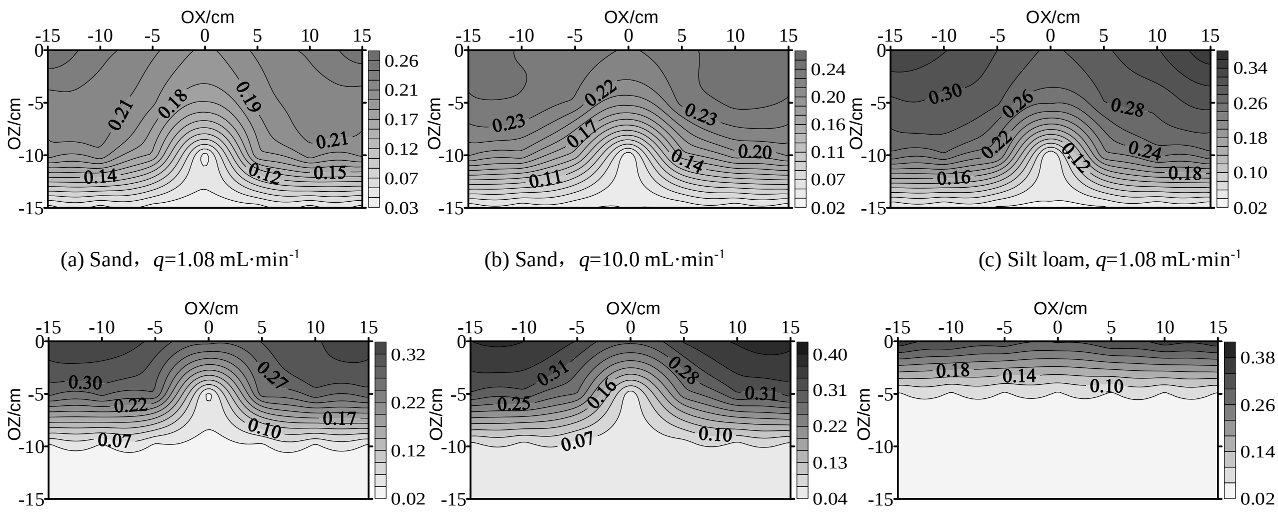

(a) Sand, q=1.08 mL·min[-1] (b) Sand, q=10.0 mL·min[-1] (c) Silt loam, q=1.08 mL·min[-1]

(d) Silt loam, q=5.0 mL·min[-1] (e) Loam soil, q=1.08 mL·min[-1] (f) Loam soil, q=5.0 mL·min[-1]

Fig. 5 Contour maps of θ on XOZ block for the three tested soils at various q after TTI.

For sand, the increment of WDPTs after trickle irrigation was not obvious at all q values. There was small increment of WDPTs for silt loam at different application rates. The increment of WDPTs for loam soil was the largest among the three tested soils.

The increments of WDPT for the whole wetted zone: The increments of WDPTs of the whole wetted zone at different q values for various soils are listed in Table 8. The $WDPT_{max}$s and $WDPT_a$s were larger than the initial conditions at various q values for loam soil. The increment of WDPTs for

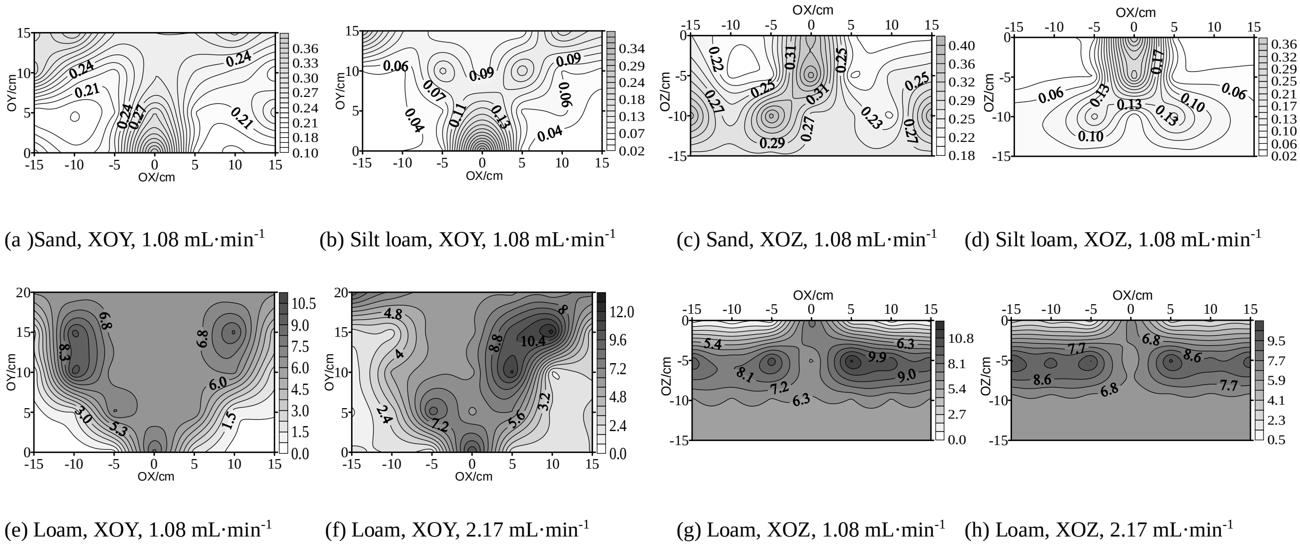

(a) Sand, XOY, 1.08 mL·min^{-1} (b) Silt loam, XOY, 1.08 mL·min^{-1} (c) Sand, XOZ, 1.08 mL·min^{-1} (d) Silt loam, XOZ, 1.08 mL·min^{-1}

(e) Loam, XOY, 1.08 mL·min^{-1} (f) Loam, XOY, 2.17 mL·min^{-1} (g) Loam, XOZ, 1.08 mL·min^{-1} (h) Loam, XOZ, 2.17 mL·min^{-1}

Fig. 6: Contour maps of soil salt content on XOY and XOZ planes for the tested soils.

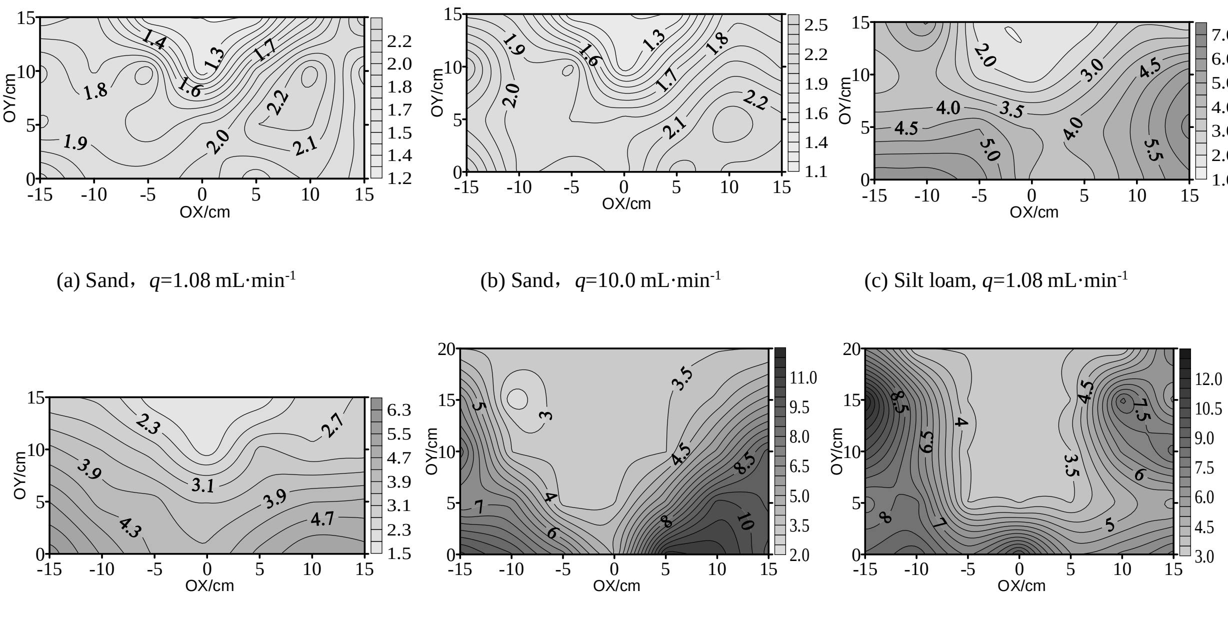

(a) Sand, q=1.08 mL·min^{-1} (b) Sand, q=10.0 mL·min^{-1} (c) Silt loam, q=1.08 mL·min^{-1}

(d) Silt loam, q=5 mL·min^{-1} (e) Loam soil, q=1.08 mL·min^{-1} (f) Loam soil, q=5 mL·min^{-1}

Fig. 7: Contour maps of WDPTs (s) for the three tested soils at various q after TTI.

sand was not apparent because both $WDPT_{max}$s and $WDPT_a$s were < 5 s. The $WDPT_{max}$s for silt loam were >5 s for all the four q values, thus its SWR level shifted to level 1. The $WDPT_a$s for silt loam were < 5 s. The $WDPT_{max}$s for loam soil were all > 10 s at three q values, thus the SWR level shifted to level 2. The $WDPT_a$s for loam soil were all > 5 s. The largest WDPTs were 11.7, 23.8 and 10.1 s corresponding to q of 1.08, 2.17 and 5.0 mL·min^{-1}. Generally, at the same q, WDPTs of loam soil varied most obviously. The "WDPT was not absolutely induced by a larger q. For given soil, the average and $WDPT_{max}$s tended to be constant, which was clear for non-saline soil.

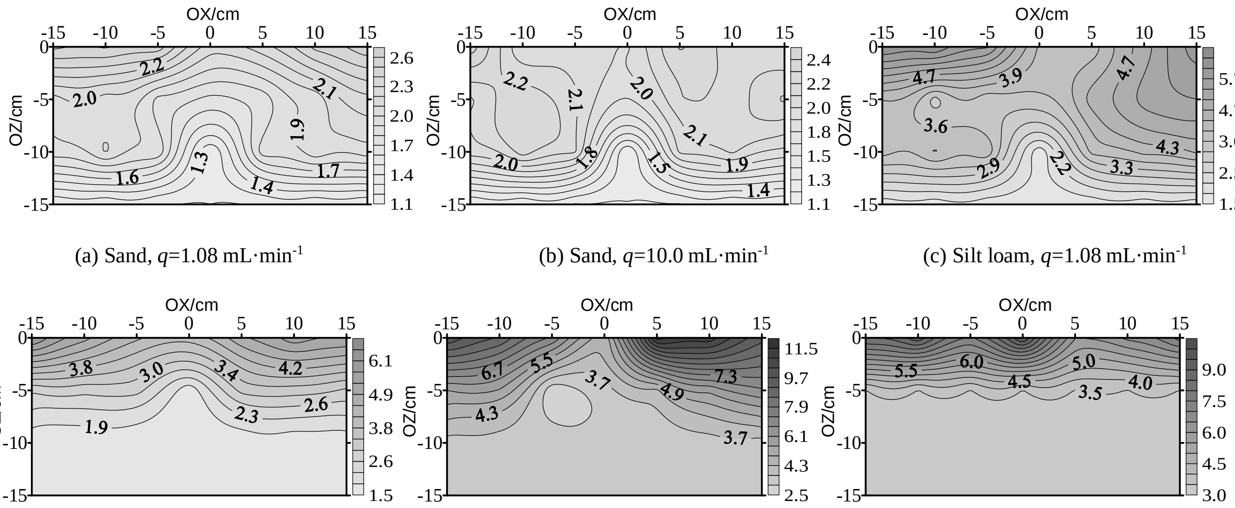

(a) Sand, q=1.08 mL·min^{-1} (b) Sand, q=10.0 mL·min^{-1} (c) Silt loam, q=1.08 mL·min^{-1}

(d) Silt loam, q=5.0 mL·min^{-1} (e) Loam soil, q=1.08 mL·min^{-1} (f) Loam soil, q=5.0 mL·min^{-1}

Fig. 8: Contour maps of WDPTs in XOZ block for the three tested soils after TTI.

WDPT variations with soil water content and soil EC: The distributions of WDPTs for different soils were generally similar to that of θ, both in XOY and XOZ blocks for all the three tested soils, which inspired us to find further connections among these three soil properties. Variations of WDPT, θ and W are shown in Fig. 9. WDPT increased as θ increased, but with different amplitude, which was applicable to all of the three tested soils at various q values. The increasing of WDPT with θ was most obvious for loam soil, followed by silt loam and sand. WDPT decreased as W increased for loam soils, because its range of soil salt content was much wide after TTI. As W was smaller than 5.0 g·kg^{-1}, WDPT decreased rapidly. WDPT decreased slowly as W increased continuously, when W was larger than 5.0 g·kg^{-1}.

DISCUSSION

TWW irrigation was shown to lead to the development of SWR. A 6-year period of recovery with no irrigation was insufficient to eliminate the induced SWR (Mataix-Solera et al. 2011). Wallach et al. (2005) reported SWR development after 20 years of irrigation with TWW. Highly spatial variability of SWR was found by Taumer et al. (2005) in a former sewage field irrigated by untreated wastewaters during 90 years. Also, short-term wastewater irrigation could lead to significant increase of SWR. According to Zupanc & Zupancic (2010), soils planted with *Populus deltoides* showed increased water repellency after irrigated with different concentrations of landfill leachate and compost wastewater, tap water and nutrient solution for 11 weeks, comparing to the original substrate. Travis et al. (2010) demonstrated that raw artificial grey water significantly increased the development of hydrophobicity in the sand and loam soils within only 40 days. Our research showed an increase of WDPT after very short (< 1 day) TTI.

Leaching the loamy and clay soils with effluent that contained high concentrations of suspended solids led to a significant reduction in hydraulic conductivity, caused by trapping of more suspended solids in the large numbers of small pores in these soils (Lado & Ben-Hur 2009). Reduction in hydraulic conductivity was consistent to the WDPT increase, although the factors influencing soil water infiltration are very complicated.

The SWR status depends greatly on θ, increased as θ is low, and decreases as θ increases to a value beyond which the soil shows no repellency (Dekker & Ritsema 1994; Dekker et al. 2001). The relationship of θ with WDPT in this research (Fig. 9) didn't totally support the above opinion. The increase of WDPT with the increased θ may be caused by two reasons. First, the soil samples were taken after redistribution of 2 hours, with wetting and drying process existed, and the hysteresis effect may influence the θ~WDPT curves. Second, soil with high θ may contain more soluble organic carbon, which was considered the main reason why soil repels water.

CONCLUSIONS

After the TTI and soil water redistribution at different application rates (q), the width - depth ratio (R_w) for sand were

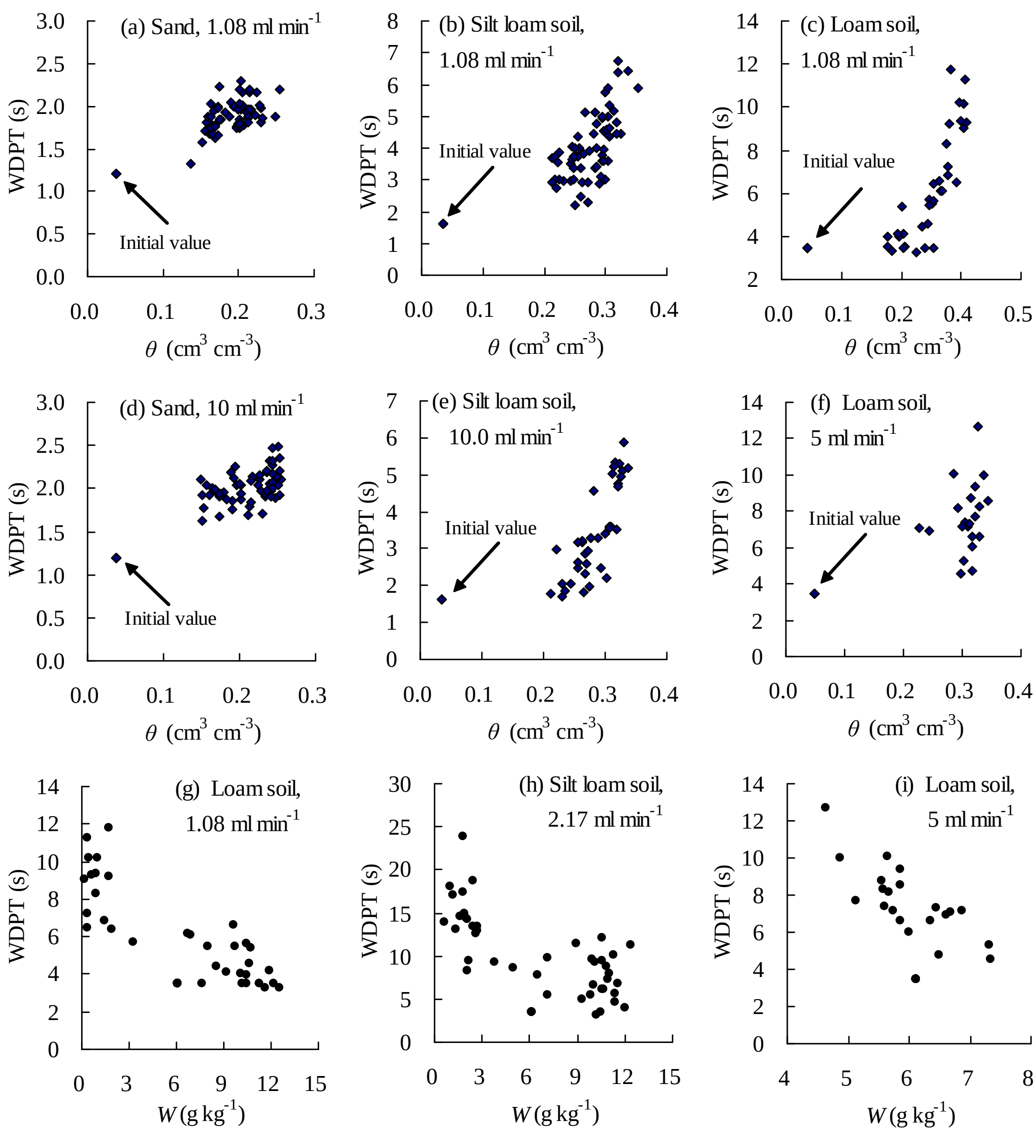

Fig. 9: Variations of WDPT versus θ and W for various application rates and soils.

around 1. The $R_w \sim t$ relationship was described as power function both for silt loam and loam soils. The WDPTs for the three soil types increased, which was most obvious for loam soil with the largest WDPT increment of 23.8 s at q of 2.17 mL·min^{-1}.

The wetted zone appeared to be a circle for sand and an ellipse for silt loam, a larger q promoted soil water infiltration to the deep-layer. Water in sand infiltrated fast, followed by silt loam. A q of 10.0 mL·min^{-1} or larger could be applied to field trickle irrigation for sand and silt loams. Water was difficult to infiltrate to loam soil as water apt to pond on the surface. It was suitable with small q (for example 1.0 mL·min^{-1} or smaller) for field trickle irrigation of loam soil. The distributions of soil salt content and WDPT were in highly consistent with those of θ. WDPT increased with the increase of θ, but decreased with the increase of W.

ACKNOWLEDGEMENTS

This research is supported by The National Natural Science Foundation of China (51579213).

REFERENCES

Al-Hamaiedeh, H. and Bino, M. 2010. Effect of treated grey water reuse in irrigation on soil and plants. Desalination, 256: 115-119.

Al-Nakshabandi, G. A., Saqqar, M.M., Shatanawi, M. R., Fayyad, M. and Al-Horani, H. 2007. Some environmental problems associated with the use of treated wastewater for irrigation in Jordan. Agricultural Water Management, 34: 81-94.

Bar-Yosef, B. and Sheikholslami, M.R. 1976. Distribution of water and ions in soils irrigated and fertilized from a trickle source. Soil Science Society of America Journal, 40(4): 575-582.

Bisdom, E.B.A., Dekker, L.W. and Schoute, J.F.T. 1993. Water repellency of sieve fractions from sandy soils and relationships with organic material and soil structure. Geoderma, 56: 105-118.

de Jonge, L.W., Jacobsen, O.H. and Moldrup, P. 1999. Soil water repellency effects of water content, temperature and particle size. Soil Science Society of America Journal, 63(3): 437-442.

Dekker, L.W. and Ritsema, C.J. 1994. How water moves in a water repellent sand: I. Potential and actual water repellency. Water Resources Research, 30(9): 2507-2517.

Dekker, L.W., Doerr, S.H., Oostindie, K., Ziogas, A.K. and Ritsema, C.J. 2001. Water repellency and critical soil water content in a dune sand. Soil Science Society of America Journal, 65: 1667-1674.

Diehl, D., Bayer, J.V., Woche, S.K., Bryant, R., Doerr, S.H. and Schaumann, G.E. 2010. Reaction of soil water repellency to artificially induced changes in soil pH. Geoderma, 158: 375-384.

Doerr, S.H. and Thomas, A.D. 2000. The role of soil moisture in controlling water repellency: new evidence from forest soils in Portugal. Journal of Hydrology, 231-232: 134-147.

Lado, M. and Ben-Hur, M. 2009. Treated domestic sewage irrigation effects on soil hydraulic properties in arid and semiarid zones: A review. Soil & Tillage Research, 106: 152-163.

Li, J., Zhang, J. and Rao, M. 2004. Wetting patterns and nitrogen distributions as affected by fertigation strategies from a surface point source. Agricultural Water Management, 67: 89-104.

Li, Y. and Shang, Y. 2016. Distributions of water droplet penetration time and soil properties under point source trickle irrigation using treated wastewater. Nature Environment & Pollution Technology, 15(3): 805-816.

Luo, J.X. 1986. Improvement of Salinity Land in Xinjiang Province. Beijing, China Water-Power Press, pp. 348 (in Chinese).

Mataix-Solera, J., García-Irles, L., Morugán, A., Doerr, S.H., Garcia-Orenes, F., Arcenegui, V. and Atanassova, I. 2011. Longevity of soil water repellency in a former wastewater disposal tree stand and potential amelioration. Geoderma, 165(1): 78-83.

Rusan, M.J.M., Hinnawi, S. and Rousan, L. 2007. Long term effect of wastewater irrigation of forage crops on soil and plant quality parameters. Desalination, 215: 143-152.

Taumer, K., Stoffregen, H. and Wessolek, G. 2005. Determination of repellency distribution using soil organic matter and water content. Geoderma, 125: 107-115.

Travis, M.J., Wiel-Shafran, A., Weisbrod, N., Adar, E. and Gross, A. 2010. Greywater reuse for irrigation: effect on soil properties. Science of the Total Environment, 408: 2501-2508.

Wallach, R., Ben-Arie, O. and Graber, E.R. 2005. Soil water repellency induced by long-term irrigation with treated sewage effluent. Journal of Environmental Quality, 34: 1910-1920.

Zupanc, V. and Zupancic, M. 2010. Changes in soil characteristics during landfill leachate irrigation of Populus deltoids. Waste Management, 30: 2130-2136.